

CASSINI MANEUVER EXPERIENCE: FINISHING INNER CRUISE

Troy D. Goodson, Donald L. Gray, Yungsun Hahn, and Fernando Peralta
Jet Propulsion Laboratory and California Institute of Technology

ABSTRACT

The Cassini-Huygens spacecraft was launched in 1997. It is an international effort to study the Saturnian system. Cassini's interplanetary cruise, which will deliver the spacecraft to Saturn in 2004, is making use of multiple propulsive maneuvers, both statistical and deterministic. The inner cruise maneuvers have been completed. The system has performed better than pre-launch expectations and requirements. Improvements to the system have been made and more accurate maneuver execution error models have been determined, based on this in-flight data. This new model will provide more realism to predictions of the fuel required to navigate the tour of Saturn's system.

INTRODUCTION

The Cassini-Huygens program is an international effort to study the planet Saturn and its moons with an orbital tour. The European Space Agency's (ESA)

Huygens probe will be delivered to Saturn's moon Titan by the Cassini spacecraft. This is the first mission to visit Saturn since the flybys made by the two historic Voyager spacecraft in 1980 and 1981. Cassini will arrive at Saturn in 2004, the climax of a long journey. Previous papers [1,2] reported prelaunch plans and experience during early cruise. Now that the inner-solar-system phase of cruise has finished, further operational experience of the Cassini mission is reported, with a focus on the deep space maneuver and subsequent trajectory correction maneuvers (TCMs). A second focus is the analysis of Cassini's maneuver execution error statistics. Armed with more accurate statistics, the navigation team can make more accurate predictions of future ΔV usage.

The interplanetary trajectory to Saturn requires four gravity-assists, two from Venus, one from Earth, and another from Jupiter. This trajectory, referred to as 97 VVEJGA, is depicted below, in Figure 1, for the actual launch on 15 October, 1997, at the opening of the daily launch window.

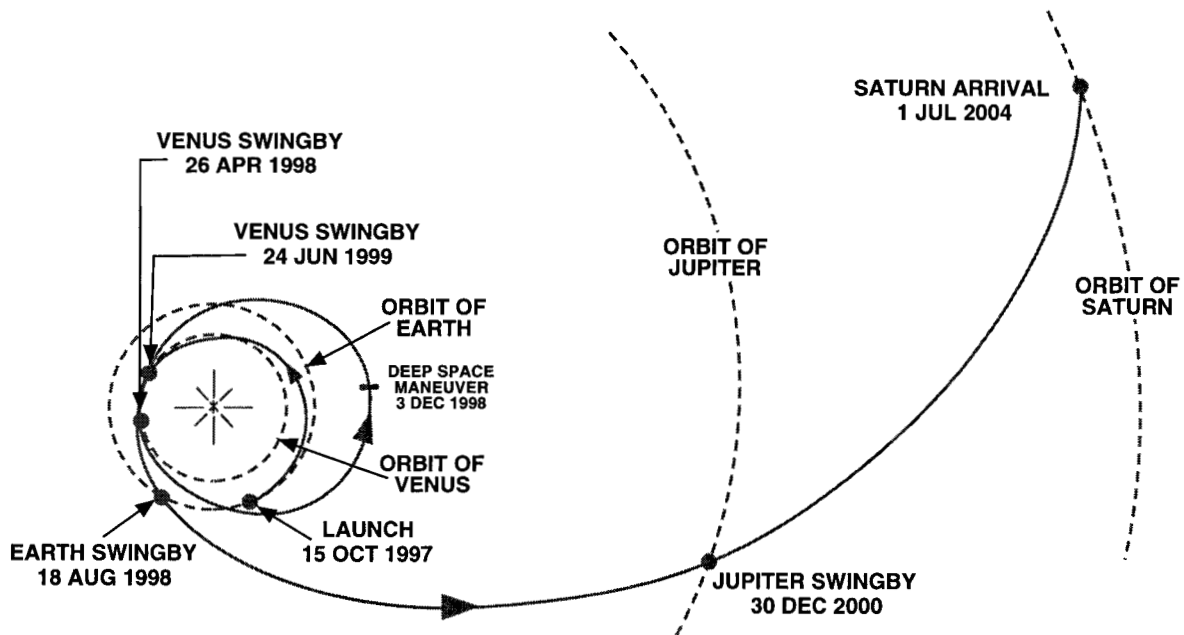


Figure 1: Interplanetary Trajectory

There are seven years between launch and arrival at Saturn. There are roughly 6.5 months between launch and the

first Venus swingby, 14 months between the two Venus swingbys, and 55 days between the second Venus swingby

and the Earth swingby. The Jupiter swingby is about one-third of way into the subsequent 5 years. There are many activities to be accomplished within this time, including the execution of up to 21 TCMs.

The previous paper [2] concluded with mention of a trajectory redesign. That redesign obviated two maneuvers by accepting the current trajectory best estimate as the start of a new reference trajectory and redesigning the downstream events and maneuver targets to accommodate it. [3] After the large Deep Space Maneuver (DSM), detailed below, another trajectory redesign was performed. [4] Again, the current best estimate became the reference and all downstream events and maneuver targets changed. Only the results of this most recent redesign are reported.

The previous paper also reported on the emerging design of TCM-5t, a test maneuver. The purpose of TCM-5t was to characterize the propulsion system by simulating conditions that would be seen later in cruise. However, after some further study these conditions proved to be more difficult to attain than expected. One particular complication was in the strategy for heating the spacecraft's propulsion system to reflect conditions somewhat closer to the sun; in fact, a suitable strategy for this heating was not found. The so-called test maneuver was cancelled.

A total of twenty-one maneuvers enter into the navigation strategy for 97 VVEJGA. The first two of these maneuvers were reported in the previous paper along with the cancellation of the third and fourth maneuvers. Several of the remaining TCMs during cruise and the final approach to Saturn are deterministic, viz. have a non-zero mean ΔV . For the most part, these deterministic components were designed in support of the Earth Swingby Plan [5]; they remove, in piecemeal, a built-in trajectory bias of the Earth swingby aimpoint. The trajectory bias was implemented by specifying targets in Earth's B-plane for the maneuver sequence from the TCM-9 to TCM-12

In addition to biasing in the B-plane, the time-of-arrival for the Earth swingby was altered with each maneuver. The time-of-arrival targets were specified to reduce the ΔV cost of the strategy. If a given bias-removal maneuver was not executed, both the B-plane aimpoint and the time-of-arrival would have been in error.

The post-Venus-1 redesign turned the current best estimate of the trajectory into the reference trajectory. A study of how this redesign would affect the Venus-2 delivery dispersions prompted a reconsideration of the post-DSM/pre-Venus-2 trajectory segment for the Earth Swingby analysis. As a result, a bias was introduced into the Deep Space Maneuver (DSM) design which would be removed by TCM-7. TCM-6 and TCM-8 would remain unbiased clean-up

maneuvers.[3]. The final sequence of bias-removal aimpoints for the Earth swingby are depicted graphically in Figure 2 and listed in Table III.

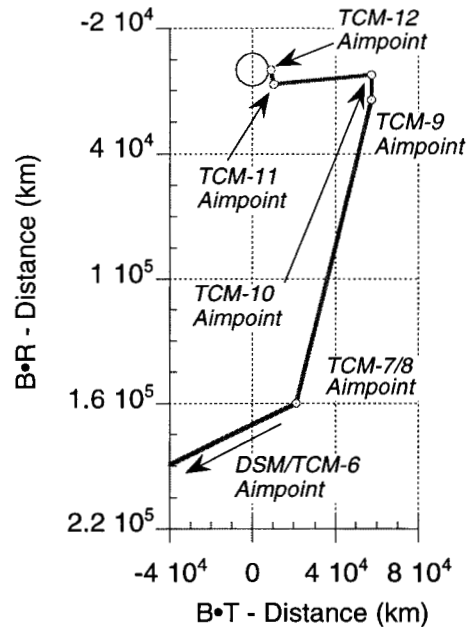


Figure 2: Aimpoint Biasing Strategy for Earth (Earth B-Plane)

The post-DSM redesign maintained the pre-Venus bias. However, this time the bias removal was split between TCM-6 and TCM-7 in such a way that TCM-6 maintained the same Earth B-plane target as the DSM but the Earth TCA target changed, as listed in Table V. In this way, TCM-7 was small enough to be performed with the monopropellant system. TCM-8 remained an unbiased clean-up maneuver.[4]

Maneuver Execution

The Cassini's Propulsion Module Subsystem (PMS) consists of a bipropellant element, the main engine, for large trajectory corrections and a monopropellant element, the Reaction Control Subsystem (RCS), for small trajectory corrections, attitude control functions, and reaction wheel desaturation. [6]

The RCS is used for small maneuvers, viz. less than 1 m/s. The RCS consists of 4 hydrazine thruster clusters – a total of 8 primary and 8 backup thrusters. These small, monopropellant thrusters supply about 0.98 Newtons each when fully pressurized and an I_{sp} of about 195 seconds. They are labeled in Figure 4. The thrusters may be grouped into two sets. The first set faces the $\pm Y_{S/C}$ spacecraft directions; it is used to make balanced turns about the $Z_{S/C}$ axis (roll turns). The other set faces the $-Z_{S/C}$ axis and is used to make

unbalanced turns about the $X_{S/C}$ axis (pitch turns) and/or $Y_{S/C}$ axis (yaw turns).

Table I: Interplanetary ΔV estimates, m/s

#	det.	Mean	sig	95%
DSM	449.97	450.02	1.52	452.56
TCM-6		11.67	0.04	11.74
TCM-7	0.24	0.54	0.27	1.08
TCM-8		0.05	0.03	0.10
TCM-9	47.33	52.01	11.82	75.44
TCM-10	5.04	5.08	0.29	5.55
TCM-11	36.89	36.89	0.15	37.12
TCM-12	12.38	12.39	0.56	13.33
TCM-13		30.48	15.96	61.1
TCM-14		.92	.76	2.39
TCM-15		.13	.06	.23
TCM-16		.16	.08	.30
TCM-17		1.51	.79	2.96
TCM-18	0.50	.58	.13	0.84
TCM-19	0.50	.55	.09	0.73
TCM-20	1.00	1.39	.42	2.21
TCM-21		.33	.16	.63

"det."=deterministic, "sig"=sigma or standard deviation, "95%" indicates that 95% of the time, the maneuver will be less than listed

Large maneuvers are executed with the main engine, which has two redundant nozzles (MEA, MEB). The two nozzles are mounted side by side along the Y-axis, which can be seen in Figure 3. Since either of these must thrust toward the spacecraft center of gravity, the resulting thrust direction has a small offset from the -Z-axis direction (approx. 7.2° or 0.13 rad). When fully pressurized, this system has a thrust of 445 Newtons and an I_{sp} of about 304 seconds.

Maneuvers, by and large, are executed in the blow-down, non-pressure-regulated, configuration. Only large maneuvers, such as the DSM and SOI, were to be executed with the regulator active. TCM-1 was to be the only exception; however, TCM-1 was executed blow-down due to concern over a regulator leak. A fuel-side-only repressurization of the system in-between maneuvers was enacted after TCM-9.

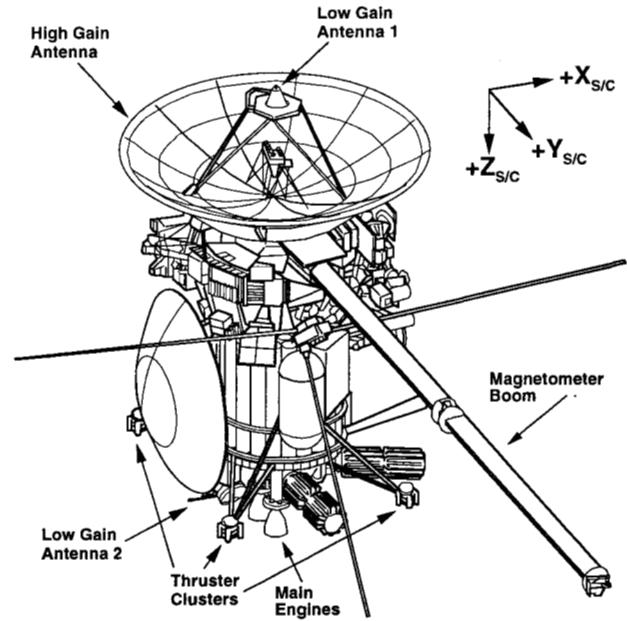


Figure 3: Cassini Spacecraft Diagram

Maneuvers are executed in a turn-and-burn manner. Prior to all main engine maneuvers, the attitude-control deadband is reduced from 20 mrad to 2 mrad (0.1°).[7] The spacecraft then performs the so-called wind turns, a roll turn about the $Z_{S/C}$ axis followed by a yaw turn about the $Y_{S/C}$ axis. These turns are designed to place the main engine (body-fixed) thrust vector along the desired burn ΔV . After the burn is complete, the roll and yaw sequence is performed in reverse; these are called the unwind turns.

In addition to the roll and yaw turns, some maneuvers include a third turn that is referred to herein as the pointing-bias-fix turn*. It is included in both the wind and unwind sets. This turn is described in more detail, below. Also, the attitude control system has been observed contributing some extra RCS firings for a very small ΔV , less than 1 mm/s, after each maneuver.

The RCS $+Z_{S/C}$ -facing thrusters do not have $-Z_{S/C}$ -facing counterparts, they are unbalanced. As a result, each maneuver has several ΔV s associated with it, including deadband tightening, roll and yaw turns, pointing bias fix turns, the burn, and the post-maneuver RCS firings. Strictly speaking, the total ΔV is the sum of all these; however, herein total ΔV refers to all but the post-maneuver firing. The burn & turns ΔV is the sum of the burn ΔV and the roll and wind turn ΔV .

* The flight team often refers to this maneuver as the 7OFFSET turn, after the flight software command used to execute it. However, a 7OFFSET command is more general and is used for other purposes, so it is referred to here as the pointing bias fix.

The total ΔV is useful for discussing the whole execution error while the burn & turns ΔV is useful in comparing with the AACCS results. See Figure 4.

Errors in all of these events contribute to the total maneuver execution error. Execution performance is primarily dependent upon performance of the on-board accelerometer and the attitude control system performance. The latter is very dependent upon pre-aiming the main engine. If the pre-aim is incorrect, the main engine is pointed such that its thrust produces a torque upon the spacecraft. The attitude control system works to remove this torque and to orient the spacecraft so that the main engine thrust vector matches the desired burn direction.

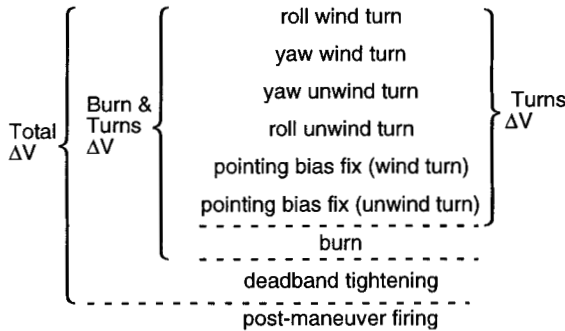


Figure 4: Definitions

Execution errors are modeled using the Gates model.[8] The Gates model accounts for four independent error sources, two each for magnitude errors and pointing errors. These are either fixed errors or proportional. Each parameter represents the standard deviation for that error source and each error source is assumed to have zero mean.

Maneuvers are forecast and, once executed, judged according to the levied execution error requirements. The pre-launch requirements are listed in Table II.

One may compute execution errors by simply subtracting the expected from the actual ΔV , but most of the insight into the source of the error comes after judiciously choosing a coordinate system to represent it with. Each maneuver ΔV is in a different inertial direction, but is controlled by spacecraft on-board systems, the accelerometer and attitude control system. It makes sense, then, to use a body-fixed coordinate system instead of an inertial system when analyzing the errors. A coordinate system definition, referred to as spacecraft coordinates $X_{S/C}$, $Y_{S/C}$, and $Z_{S/C}$, already exists for Cassini and is denoted in Figure 3. The $Z_{S/C}$ axis points from the high-gain antenna to the main engine, the $Y_{S/C}$ axis points away from the probe, and the $X_{S/C}$ axis completes the right-handed system.

Table II: TCM Error Requirements (3- σ)

System	Magnitude		Pointing	
	Fixed	Prop. (%)	Fixed	Prop.
RCS	10.5	6	10.5	25.5 mrad
MEA	30 [†] , 50 [‡]	1 [†] , 3 [‡]	52.5 [†] , 105 [‡]	20 mrad [§]

However, a coordinate system with an axis parallel to the expected ΔV is preferred. The compromise is a coordinate system with Z parallel to the expected ΔV , X parallel to the projection of $X_{S/C}$ into the plane perpendicular to Z, and Y completes the right-handed system. The plane perpendicular to Z is referred to herein as the pointing plane.

MANEUVER EXPERIENCE

After TCM-2, two flight software corrections were made, both relating to the accelerometer. The accelerometer scale factor was in error by 1%, biasing the system to overburn by that amount. The other correction was one made to the algorithm which compensates for the misalignment between the accelerometer mounting and the thrust vector. This potentially reduced burn magnitude error by as much as 0.8%. These two corrections are credited with the excellent magnitude errors discussed below.

DSM

The Deep Space Maneuver (DSM) was the largest that this spacecraft will execute prior to the Saturn Orbit Insertion (SOI) in 2004. The DSM was also the only maneuver for which the propulsion system was fully pressure-regulated and no other maneuver will be fully pressure-regulated until the SOI.

*Given in mm/s

[†]Uncalibrated (TCM-1, TCM-2, and SOI)

[‡] Calibrated

[§] For long burns, such as the DSM and SOI, this requirement is relaxed to 30mrad. However, high quality gyros were procured and the star sensor remains in use during the burn, making the relaxation unnecessary.

Table III: Trajectory Events, Including Maneuvers and Targets

Event	Date of Event (UTC)		Targets			
			Body	B•R (km)	B•T (km)	TCA (UTC)
Launch	15-Oct-1997					
TCM-1	9-Nov-1997	20:00:00	Venus	-1910	12302	13:44:49
TCM-2	25-Feb-1998	20:00:00	Venus	-1910	12302	13:44:49
Venus-1 Flyby	26-Apr-1998	13:44:49	Venus	-1910	12302	13:44:49
DSM	3-Dec-1998	6:00:00	Earth [*]	1121120	-1978790	18:31:47
TCM-6	4-Feb-1999	20:00:00	Earth [†]	1121120	-1978790	17:04:39
TCM-7	18-May-1999	20:00:00	Earth	160000	21210	3:42:22
TCM-8 [‡] (V2-14d)	10-Jun-1999	18:00:00	Earth	160000	21210	3:42:22
Venus-2 Flyby	24-Jun-1999	18:25:20	Venus	3296	-9064	20:29:57
TCM-9	6-Jul-1999	17:00:00	Earth	14400	57510	3:28:51
TCM-10	19-Jul-1999	16:00:00	Earth	2400	57510	3:29:03
TCM-11	2-Aug-1999	21:30:00	Earth	6960	10390	3:28:38
TCM-12	11-Aug-1999	15:30:00	Earth	164	8960	3:28:25
Earth Flyby	18-Aug-1999	3:28:25	Earth	164	8960	3:28:25
TCM-13	31-Aug-1999	16:00:00	Jupiter	130523	10898129	10:36:24
Jupiter Flyby	30-Dec-2000	10:36:24	Jupiter	130523	10898129	10:36:24
Saturn Arrival	1-Jul-2004	8:40:47	Saturn	-217939	393160	8:40:47

Design characteristics for the DSM, and the following maneuvers, are listed in Table V. The cut-off date for the last radiometric data, the size of the ΔV desired, the roll, and the yaw turn angles are all listed. Additionally, the Earth-look angle is provided. The look angle is the angle between the total ΔV vector and a vector from the spacecraft to Earth. The Earth-look angle provides insight into the observability of maneuver. If the angle is zero, the vectors are aligned and the magnitude of the maneuver will be well-estimated. If the angle is close to 90° , then one component of the pointing error will be well-estimated.

As noted in Table V, the data cut-off for the DSM was well before execution. Being such a large maneuver, its design was not very sensitive to further orbit information. The additional time allowed for an extensive review and some double-checking of this important maneuver.

The execution of the DSM revealed a total ΔV pointing error of 0.89° and a burn-only ΔV pointing error of 0.94° — somewhat larger than the 0.61° previously reported for TCM-1.[2] Curiously, the AACS on-board estimate of the

pointing error was only 0.29° . On the other hand, Navigation's estimate of the magnitude error was only about 0.05%, a considerable improvement over the 1.67% for TCM-1.[2] The execution errors are summarized in Table VI and the resulting delivery errors are summarized in Table V.

The large pointing error for the DSM led to speculation as to whether the spacecraft had a pointing bias. This suspicion prompted an examination of the difference between NAV's and AACS' pointing estimates. AACS's data represents the S/C system's own estimates while NAV's data represents what was actually observed from Earth; therefore, the best place to look for a bias is not in either of these data alone, but in their difference, NAV-AACS.

The pointing error was computed for both maneuvers. The components of ΔV error along the X and Y pointing plane axes were divided by the magnitude of the maneuver, giving angular error along these axes in radians. The results may be seen in Figure 6. The ellipse around the TCM-1 estimate is the $1-\sigma$ (one sigma) uncertainty in that estimate. The same

*Equivalent to Venus; 24-Jun-1999 21:52:52 UTC, B•R 3269 km, and B•T -9775 km.

†Equivalent to Venus; 24-Jun-1999 20:30:14 UTC, B•R 3255 km, and B•T -9759 km.

‡ TCM-8 was cancelled.

was included for the DSM estimate, however the ellipse is too small to see given the scale of the plot.

That analysis revealed that the two maneuvers had similar NAV-AACS pointing errors. Also, these NAV-AACS errors were in the same quadrant of the pointing plane. This conclusion was supported by a pre-launch analysis which had indicated such a bias might exist. [9]*

Table V: Summary of of Maneuver Design Characteristics

	Data Cutoff		ΔV	Roll	Yaw	Look†
DSM	7/17	22:24	450.0	-170.7°	-89.13°	58.99°
6	1/27	14:50	11.55	-18.97°	-10.71°	33.66°
7	5/7	9:53	0.2386	-163.6°	-110.1°	46.00°
9	6/27	18:12	43.54	-79.33°	-115.3°	81.33°
10	7/13	17:40	5.133	-80.74°	-93.29°	90.03°
11	7/27	17:40	36.31	-171.7°	-64.86°	92.01°
12	8/7	09:55	12.26	-84.76°	-88.37°	92.58°
13	8/24	17:39	6.710	8.63°	-83.19°	93.11°

Times are UTC, dates are month/day, and ΔV is m/s

To correct the bias a new rotation of the spacecraft was introduced into the maneuver sequence. This new turn would occur just after the yaw-wind turn and it would be undone just before the yaw-unwind turn. However, the ΔV due to this turn, about 7.6 mm/s, was ignored in the maneuver design.

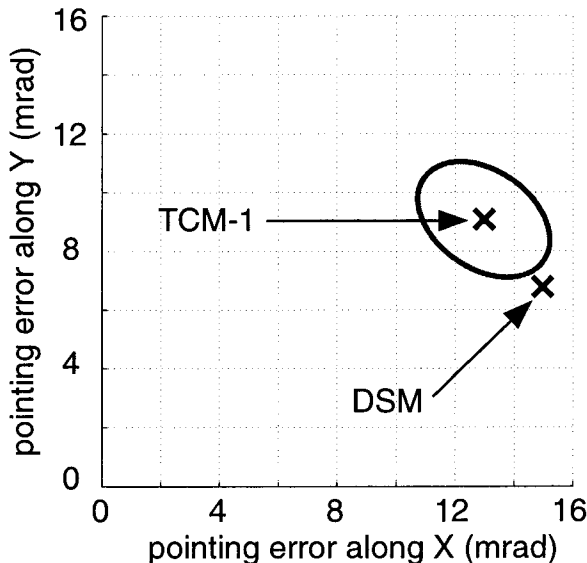


Figure 6: Indication of Maneuver Pointing Bias in Pointing Error Measurements of TCM-1 and

* The bias had been ignored because it was smaller than the 3- σ requirement listed in Table II.

† The look angle listed is the angle between the total ΔV vector and a vector from the spacecraft to Earth.

DSM. Pointing Errors, as Angles, for TCM-1 and the DSM

Curiously, the NAV-AACS pointing error for TCM-2 was similar to that for TCM-1 and the DSM, but TCM-2 used the monopropellant system and had been the only maneuver to do so up to that time. There was no pre-launch analysis supporting an RCS pointing bias and it was decided to wait for more RCS results before taking any action.

TCM-6

TCM-6 was originally planned as a purely statistical maneuver, a clean-up, and in the unlikely event that the DSM had small enough execution errors, it could be cancelled. The trajectory redesign changed those plans and, therefore, the procedure for designing this maneuver. The best-estimate the post-DSM orbit was used by the CATO optimization software to devise new Venus-2, Earth, and Jupiter swingby and time-of-closest-approach targets while holding constant the Earth-bias-removal strategy. The B-plane targets for TCM-6 were part of the Earth-bias-removal strategy and, therefore, not changed. The target for time of closest approach with Earth for TCM-6 was changed. The final target parameters for TCM-6 are listed in Table III.

The roughly 7 m/s error from the DSM would require about 12.6 m/s to fully correct with TCM-6. However, by optimizing TCA targets, this was reduced to about 11.6 m/s.

The direction of the DSM ΔV error helped TCM-6 have a very favorable viewing geometry. Each ΔV event that made up TCM-6 was observable with radiometric Doppler data. Even though the only well-determined component of each ΔV was along the vector between the spacecraft and Earth (the line-of-sight), this information was very valuable.

Table V: Maneuver B-Plane Delivery Errors

#	B•R	B•T	TCA	SMAA	SMIA	θ	σ_{TF}
DSM							
6	-460e3	15e3	7830	60e3	6e3	34°	2060
7	18e3	14e3	1259	8	8	52°	0.2
9	275	96	15	49	4	87°	0.008
10	-97	3	1	31	8	80°	0.005
11	-84	-280	2	6	2	74°	0.004
12	3	9	0.6	6e-4	5e-4	79°	4e-5
13	-870	-246	-1677	400	200	54°	100

Errors are (estimate-design); B•R, B•T, SMAA, and SMIA are in km; and TCA and σ_{TF} are in seconds.

TCM-13 is Jupiter B-plane, others are Earth.

‡ The hyperbolic excess speed for the Venus-2 swingby was about 9.4 km/s. $(4*3600 \text{ s} + 50*60 \text{ s})*9.4 \text{ km/s} \approx 163,000 \text{ km}$.

The navigation team was able to estimate how the individual ΔV errors contributed to the total B-plane delivery error. The breakdown for the Venus-2 B-plane is shown in Figure 7. In that figure, it is clear that OD error and maneuver execution error played almost equal roles in determining the delivery error. One can also see that the sum of the contributions of the dead-band tightening ΔV and the pointing-bias-fix turn ΔV are greater than the burn error. Assuming that the errors in TCM-6 are typical, then there is considerable improvement to be had by modeling the dead-band tightening ΔV and the pointing-bias-fix turn ΔV .

Reducing OD errors is more challenging. The OD drift in Figure 7 is broken down into pre- and post-maneuver. However, together they represent the convergence of the OD solution from the pre-maneuver estimate to the post-maneuver reconstruction. The point labeled A represents the best estimate available when the maneuver was designed on January 27th. Not counting the weekend, five working days were used to write, test, and upload the maneuver sequence to the spacecraft. The point at the other end of the line segment B represents the best estimate available when the maneuver was executed on February 4th. The point labeled J is the best estimate available 21 days later. If the maneuver had been designed and executed on February 4th, then there would have been no pre-maneuver OD error and line segment B would disappear from the diagram. Therefore, those five workdays for developing the sequence had a real cost in delivery accuracy. Furthermore, if the whole process had been shifted later, then the best-estimate used for the design would have been better, reducing all OD errors. On the other hand, this pre-maneuver drift is also attributable to an underestimation of the uncertainty in maintenance activity ΔV 's that occurred between the DSM and TCM-6. This maintenance activity was called the Instrument Check Out and further discussion of the OD issues surrounding it may be found in Ref. 10.

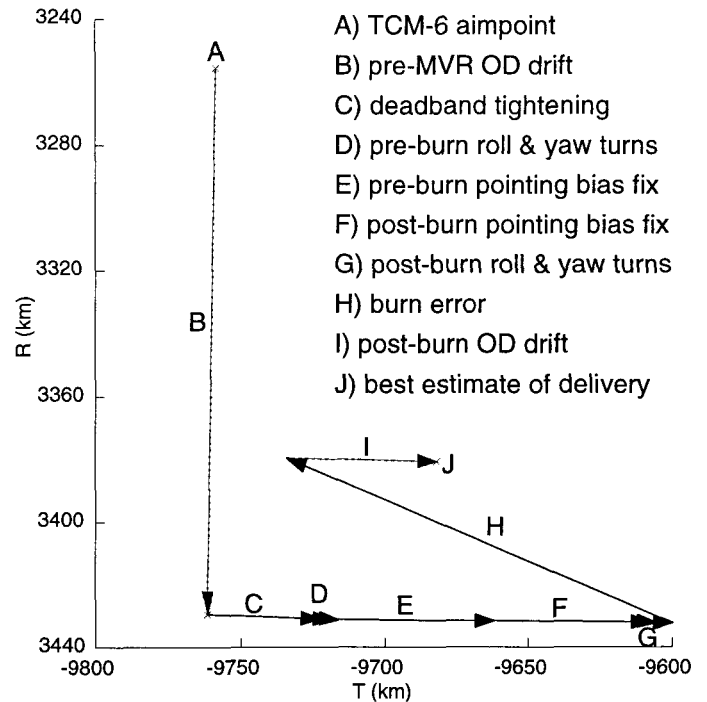


Figure 7: Various contributions to TCM-6's Venus-2 B-plane delivery error

TCM-7

Like TCM-6, TCM-7 had originally been planned as a clean-up maneuver; however, it took on a small deterministic component for the trajectory redesign. Since its deterministic component was limited to 0.25 m/s, the chances that it could be executed with the RCS instead of the main engine were kept high.

The final orbit estimate held the line so that TCM-7 did not require the main engine. TCM-7 is the second RCS maneuver the spacecraft performed. However, it owes its small size to the accurate execution of TCM-6. It, too, had favorable look-angles during the burn and is the only RCS maneuver to date where the radiometric data was collected during the burn, allowing separate estimates of burn and turn ΔV .

The pointing error estimates from TCM-7 are plotted in Figure 8. Navigation's and AACS' estimates are shown with their 1- σ uncertainty ellipses, alongside the 1- σ requirement. Navigation's estimate lies just outside the requirement, though not far from it, and is clearly inside 2- σ of the requirement. Also, this pointing error is quite unlike TCM-2's pointing error, both in size and direction. Even the difference NAV-AACS is quite unlike that seen for TCM-2. Hence, there is still little evidence for any pointing bias for RCS maneuvers.

TCM-8

The cancellation of TCM-8 was anticipated; that much is clear from Table I. When the scheduled time for TCM-8 arrived, the required B-plane shift was only 2 km and the TCA correction needed was only 2 seconds. In fact, this translated into a 4 m/s savings for TCM-9; in other words, some of the TCM-9 bias removal was already taken care of. Seeing that this difference was within the navigation delivery statistics for TCM-8, the flight team decided that the delivery could not be improved much considering the expected execution errors from TCM-8 and so the maneuver was cancelled.

Venus-2

The Venus-2 swingby occurred on June 24, 1999 at approximately 20:29:55 UTC. It was the only non-targeted swingby during interplanetary cruise. That isn't to say that the swingby wasn't necessary, but that the maneuver sequence leading up to Venus-2 aimed at points in Earth's B-plane, not Venus'.

TCM-9

The first of the post-Venus, four Earth-bias-removal maneuvers and doubling as the Venus-2 swingby clean-up, TCM-9 was scheduled for 45 days before the swingby with Earth.

TCM-9 was the first maneuver to include the 3 mm/s deadband-tightening ΔV in its design, reducing the total ΔV error by that amount.

Unfortunately, the geometry of bias to be removed was not favorable for radiometric tracking. As can be seen in Table V, the look angle for this maneuver was near 90° . Individual ΔV events could not be discerned and so the only estimates are for TCM-9 total ΔV . Furthermore, TCM-9 had a large B•R component to its bias removal, as seen in Figure 2, so that there was a large out-of-plane component to its ΔV , making the estimation of TCM-9 that much more difficult.

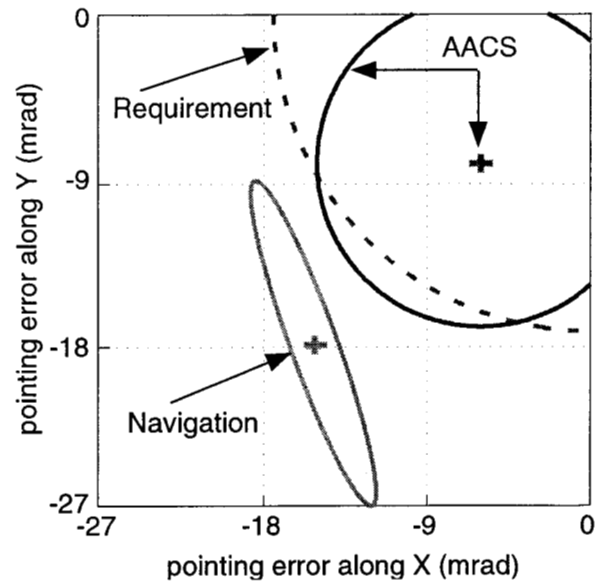


Figure 8: TCM-7 Pointing Errors in Pointing Plane

After TCM-9, the system was regulated, fuel-side only. This ensured that the bipropellant system would have acceptable operating conditions for the rest of the cruise trajectory.

TCM-10

The unfavorable geometry was a little worse for TCM-10, whose ΔV was mostly perpendicular to the trajectory plane making the orbit estimation more difficult, but entirely within mission requirements.[10] In hindsight, had more resources been available pre-launch, this geometry might have been improved.

TCM-10 was the first maneuver to include both the 3 mm/s deadband-tightening ΔV and the 7.6 mm/s pointing-bias-fix ΔV in its design. The net effect was to reduce the magnitude error by 7.6 mm/s and to reduce the pointing error by about 3 mm/s. All later maneuvers incorporated these ΔV s into their designs.

TCM-11

There was some consideration given to pre-designing, or canning-in, the design for TCM-11; the idea being that the design could be made months in advance, lightening the work load during these three months between Venus-2 and Earth. The ΔV cost would be small. On the other hand, all the ground system procedures would be different for this one maneuver. Rather than risk the confusion, TCM-11 was not canned-in; it took advantage of the same design process used for the other maneuvers.

TCM-12

Although it was not given a special moniker like the DSM or SOI, TCM-12 was one of the most important maneuvers of the whole interplanetary cruise. The trajectory bias left over by TCM-11 (as planned) would forestall the mission. The spacecraft would pass Earth at such great distance that the gravity assist would be far too weak to reach Jupiter. Furthermore, this maneuver was, by requirement, placed only six-and-a-half days before the Earth swingby.

The TCM-12 design was slightly complicated by the desire to avoid any Earth-orbiting debris. It had been decided before launch that the flight team would take account of the risk of collision with Earth-orbiting objects during the swingby. Beginning in 1998 and with more frequency in July and August of 1999, data was exchanged with the U.S. Air Force Space Command to determine if any debris hazards warranted concern.[11] Predictions showed one debris object with a closest approach distance to the spacecraft of 4 km occurring 138 seconds after the spacecraft's perigee. Although the probability of collision was low, the time of perigee was delayed 14 seconds. That delay increased the closest approach distance with the object from 4 km to about 90 km. Earth TCA listed in Table III includes the 14 second TCA shift that was implemented.

One can see in Table V, that the data cut-off for TCM-12 was much closer to the maneuver than for the prior maneuvers. This turn-around time was reduced for TCM-12 so that as much radiometric data as possible could be processed before the maneuver design, ensuring an accurate swingby.

Earth

The additional data used for TCM-12 clearly paid off, as evidenced by the small TCM-12 delivery errors listed in Table V. Further evidence is provided by the small size of TCM-13, discussed below. The statistical predictions in Table I show a mean ΔV of about 30 m/s for TCM-13, yet it only needed about 7 m/s.

Just before the swingby, Cassini's magnetometer boom was deployed. The boom is shown in Figure 4 extending towards the lower right-hand corner of the drawing.

TCM-13

Hand-in-hand with the power of the gravitational assist from Earth comes sensitivity in the swingby conditions. Even the small error incurred must be corrected as early as possible. This is clearly shown in the *a priori* expectation of 30 m/s for TCM-13.

TCM-13 also benefited from its geometry. Like TCM-6, the individual ΔV events were observable, allowing the burn to be characterized.

The pointing error in this maneuver, though only about one-third that of the DSM, is still much larger than the maneuvers immediately preceding it. That error is mostly due to an incorrect setting for the main engine pre-aim, discussed earlier. The setting failed to account for the center-of-mass shift due to the magnetometer boom*.

Table VI: Maneuver Burn Execution Errors

	Magnitude		Pointing	
	Error	1- σ	Error	1- σ
DSM	0.05%	2.8	0.890°	0.0011°
6	-0.095%	6.9	0.0773°	0.14°
7	-2.35%	0.28	1.34°	0.54
9	-0.12%	15.3	0.115°	0.005°
10	-0.05%	6.0	0.113°	0.017°
11	-0.059%	2.8	0.106°	0.011°
12	-0.087%	3.4	0.0928°	0.0044°
13	-0.38%	8.0	0.287°	0.12°

Magnitude 1- σ uncertainties are in mm/s, numbers for TCMs 9 through 12 are for total ΔV

Post Maneuver ΔV

After each of these maneuvers, Navigation noticed additional RCS thruster firings. In every case so far, these firings have been estimated separately. Strictly speaking these are execution errors, although not treated as such here, esp. as they are so small. For reference, the estimated ΔV from each such event is listed in Table VII.

Table VII: Post-Maneuver ΔV s

DSM	Not observed
TCM-6	0.32 mm/s
TCM-7	0.084 mm/s
TCM-9	0.31 mm/s
TCM-10	0.37 mm/s
TCM-11	0.17 mm/s
TCM-12	0.37 mm/s
TCM-13	1.6 mm/s

NEW EXECUTION ERROR MODEL

After observing such marvelous maneuver performance, the flight team realized that this mission might be flown with a significant savings of ΔV . The way to judge what savings is available is to use an updated maneuver execution error model

* That the magnetometer boom shifted the center-of-mass was well understood, including the magnitude of that shift. This error was a case of neglect, not miscalculation.

in forecasting and planning the rest of the mission; in other words, updating Table I. With this in mind, the Navigation team has analyzed the execution errors to date.

The maneuvers during early cruise [2], TCM-1 and TCM-2, are not included in this execution error analysis. TCM-2 is excluded because it was performed with the RCS, not the main engine. The first maneuver, TCM-1, was executed with a different accelerometer scale factor and an error in the algorithm for estimating maneuver magnitude.

The focus of this analysis is on the maneuvers during inner cruise, that is, the maneuvers performed inside the asteroid belt. This includes the Deep Space Maneuver (DSM) and TCMs six through thirteen, and barring TCM-7, all of these employed the main engine.

The spectacular maneuver performance discussed above has motivated the estimation of new Gates model parameters for maneuver execution error. With this new model in hand, more realistic ΔV estimates for the remainder of cruise and, more importantly, the tour may be made.

In the above discussion of maneuver results, execution errors were discussed in the context of what was designed versus what was actually executed. However, those designs did not necessarily take advantage of all available models. For example, the design of TCM-6 did not account for the ΔV due to deadband-tightening. The design of TCM-9 did not account for the ΔV due to the pointing-bias-fix turn. These models are, however, a part of the best-available estimates used in the *a posteriori* analysis execution error analysis, below.

The software set used for maneuver design does not model the ΔV due to the pointing-bias-fix turn, nor was the deadband-tightening ΔV included in every maneuver design. Therefore, the errors quoted in Table VI do not make use of the best available estimate for that maneuver. This analysis required that best available estimates be calculated for each maneuver. The best available estimate is made using current knowledge of the ΔV s associated with maneuvers. For example, it is only with experience that 3 mm/s has become the best estimate for the deadband tightening ΔV . No pre-launch prediction of that ΔV was made.

The DSM represents a special case because it is the only maneuver in the data set considered that was executed before the pointing bias fix. Therefore, the commanded burn ΔV must be rotated to coincide with the current best estimate of the main engine pointing direction.

The magnitude errors are listed in Table VIII. The pointing errors are listed in Table X. These errors are listed in units of speed, mm/s, as these are more natural units for estimating the Gates model parameters.

While the magnitude errors are one-dimensional and, given the small number of measurements, fairly easy to understand in a table, the pointing errors are two-dimensional and are best presented in a figure using angular units, viz. Figure 10.

Table VIII: Best Estimate Magnitude Errors

	Magnitude (m/s)	Error (mm/s)	Uncertainty 1- σ (mm/s)
DSM	449.9740	258.52	2.52
6	11.5615	-9.0421	6.73
9	43.5504	-58.856	15.3
10	5.1403	-2.6877	5.95
11	36.3182	-21.264	2.80
12	12.2642	-10.669	3.44
13	6.7185	-10.599	8.04

In perusing these data, several peculiarities are noticed. First and foremost, the DSM is the only overburn of the set and is still not understood. Also, if there were no mean fixed or proportional error, then one would expect half the samples to be underburns and half to be overburns. However, there does seem to be such a bias: a 0.1% underburn. If the DSM error were simply of the other sign, this would be a very comfortable conclusion. On the other hand, the DSM is unique enough (largest, pressure-regulated) to suspect it is truly an exception.

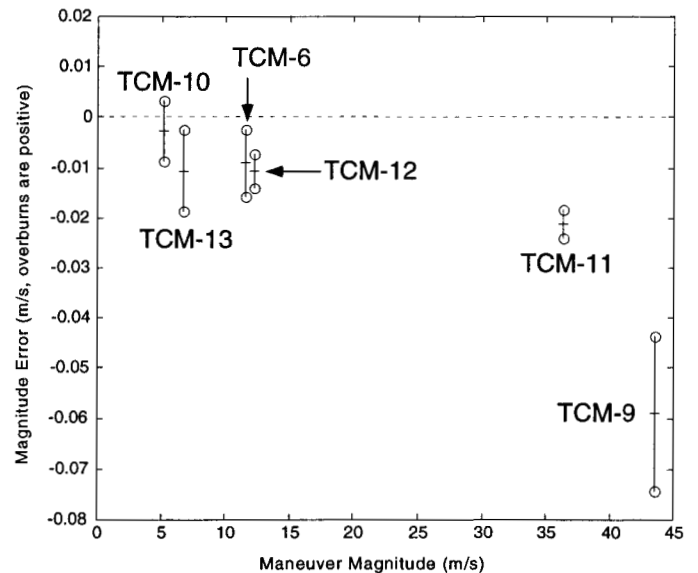


Figure 8: Magnitude errors (m/s) versus maneuver magnitude (m/s).*

* Overburns are positive, error bars indicate 1- σ uncertainties. DSM error is off scale (not shown).

The pointing error data is just as rich. First, the TCM-13 pointing error must be thrown out of the analysis because we know that the modeling did not properly reflect the magnetometer boom deployment, but it is too difficult to compute a best-estimate of the expected ΔV given that error. Second, like the magnitude data there appears to be a bias: 1.7 milliradian (0.1°) along the +Y axis in the pointing plane. On the other hand, the TCM-6 pointing error is in a different quadrant. This is still not understood; however, the prevailing assumption is that the main engine pre-aim for TCM-6 was not as good as the pre-aims for the DSM, TCM-9, TCM-10, TCM-11, and TCM-12.

Recalling that the pointing bias correction now in use was computed based on the DSM execution errors, one might expect the best-estimate DSM pointing error to be zero. Put another way: why isn't the point labeled DSM in Figure 10 at the origin? The pointing-bias correction was based on the difference between Navigation's estimates and AACs' (NAV-AACS). Since Figure 10 is based only on Navigation's estimates, the pointing error seen for the DSM is AACs' pointing error estimate.

Table X: Best-Estimates of Pointing errors

	X, m/s	Y, m/s	1- σ Uncertainty (mm/s)
DSM	0.121	0.634	$8.06 \times 4.08, 79.9^\circ$
6	0.0140	-0.00528	$28.3 \times 8.04, 114^\circ$
9	0.0395	0.0780	$6.66 \times 0.156, 8.73^\circ$
10	-9.80×10^{-5}	0.0101	$0.982 \times 0.132, 45.7^\circ$
11	0.0167	0.0650	$6.76 \times 0.143, 85.6^\circ$
12	-0.0106	0.0168	$1.29 \times 0.152, 78.6^\circ$
13	-0.00728	0.0360	$13.7 \times 0.462, 88.7^\circ$

1- σ uncertainty numbers are 1- σ ellipse dimensions with angle relative to X axis.

The four Gates model parameters mentioned earlier represent the standard deviations of four independent distributions. However, the data available is only the magnitude and pointing errors. Given that the fixed-error standard deviations are expected to be small relative to the large TCMS, they are not likely to be well-estimated using the data in hand. Therefore, no recommendations for the fixed-error parameters will be made.

Maximum Likelihood Estimation

It is not difficult to set-up a maximum likelihood estimation problem for this task. First, the probability density function (*pdf*) for the magnitude error is

$$f_m(x) = \left[2\pi(\sigma_1^2 + y^2\sigma_2^2) \right]^{-1/2} \exp \left[-\frac{1}{2} \left(\frac{x - \mu_m}{\sigma_1^2 + y^2\sigma_2^2} \right)^2 \right]$$

where x is the error, y is the magnitude of the maneuver, σ_1 and σ_2 are the fixed and proportional Gates model parameters for magnitude, and exp is the exponential function. Then, the likelihood function is defined as the product of evaluations of $f_m(x)$ for each measurement,

$$L_m(\sigma_1, \sigma_2) = \prod_{i=1}^N f_m(x_i; y_i, \sigma_1, \sigma_2)$$

A corresponding likelihood function $L_p(\sigma_3, \sigma_4)$, may be defined for the pointing error, a two-dimensional vector, whose *pdf* is

Error! Objects cannot be created from editing field codes.

where x is the length of the pointing error vector in units of speed, y is the magnitude of the maneuver, σ_3 and σ_4 are the fixed and proportional Gates model parameters for pointing, and exp is the exponential function.

A weighted maximum likelihood approach may be constructed by raising each term in the likelihood function to a power. For the magnitude errors, the exponent is the inverse of the 1- σ uncertainty. For pointing errors, the uncertainty is two-dimensional and the semimajor axis of the 1- σ uncertainty ellipse was used.

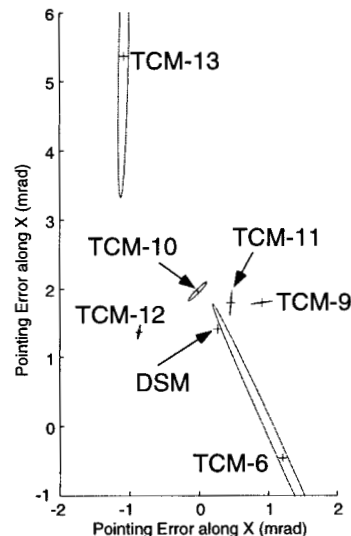


Figure 10: Best-estimates of pointing errors, shown in the pointing plane.

The Gates model parameters for magnitude errors are found by maximizing L_m ; likewise for pointing errors. Based on the form of these equations, one expects that only two measurements are required to determine the parameters. Obviously, the more measurements taken, the better these estimates of the parameters will be.

Results

The primary result of this analysis is a recommendation for Gates model parameters that more accurately represent maneuver execution errors using current maneuver modeling. These Gates model parameters will be used to update statistics for future maneuvers and for studying navigation strategies during the tour.

The secondary result is an estimate of how much improvement can be gained in execution errors by refining maneuver modeling. Obviously, this requires either some conjecture. These speculative assumptions include the following:

- the DSM magnitude error does not represent typical performance,
- the TCM-6 pointing error does not represent typical performance,
- the magnitude errors contain a -0.095% bias, and
- the pointing errors contain a 1.7 mrad bias along the $+Y$ pointing-plane axis.

The first two assumptions must be accepted in order to consider the latter two. However, all four speculations lead to considerable analysis before they can be resolved. No model has been found that might explain why the DSM was the only overburn to date. On the other, given that the DSM execution error is atypical, the -0.095% bias merely represents an error in the scale factor for the on-board accelerometer.

The TCM-6 pointing error is very suspiciously correlated with the main engine pre-aim setting. Figure 10 shows the history of main engine pre-aim settings. The feature of interest here is the TCM-6 setting, which is quite different from the other settings. It does not take a great leap of imagination to propose models of how the main engine pre-aim setting affects pointing errors in such a way to explain away the TCM-6 pointing error. On the other hand, no analysis has been performed to support any such model and so the relationship between the TCM-6 pre-aim setting and the pointing error remains speculation.

A pointing error bias along the $+Y$ pointing-plane axis, which is nearly parallel to the $Y_{S/C}$ axis in Figure 3, is even more difficult to explain. Although not shown here, the AACS estimates also indicate such a bias. One is then lead to speculate that this 1.7 mrad bias is related to the attitude control system. No analysis has been performed to support this, either.

If one accepts the above speculations, which are not unreasonable, then the way is clear to estimate the execution

error capability of the spacecraft. By simply subtracting out the -0.095% magnitude bias and the 1.7 mrad pointing bias, the remaining errors show no clear pattern and appear quite random.

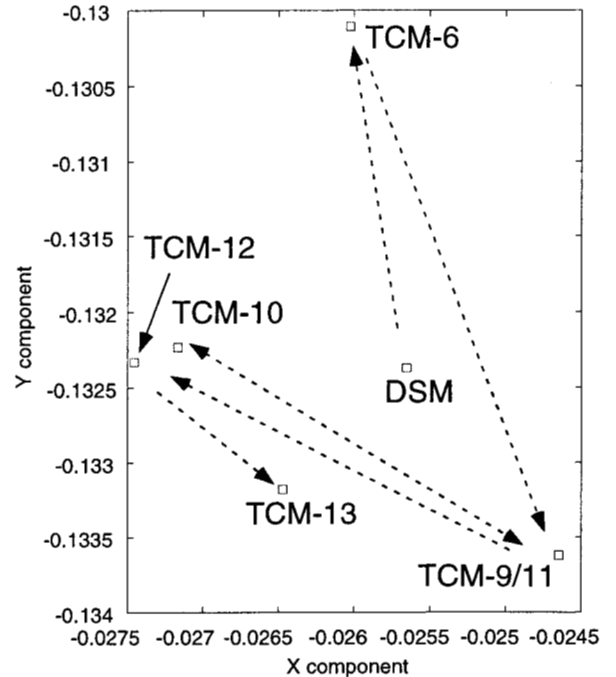


Figure 10: History of main engine pre-aim settings.

This is an ideal data-set for applying the weighted maximum likelihood estimator described above. Using FMINS from the Matlab™ analysis software, gives the following $1-\sigma$ results: (magnitude) $\sigma_1=1.8$ mm/s, $\sigma_2=0.03\%$, (pointing) $\sigma_3=2\times 10^{-6}$ mm/s, $\sigma_4=0.55$ mrad (0.032°).

Recommended Model

Finally, throwing all this speculation aside, there remains the question of what Gates model parameters best represent the errors seen in Table VIII and Table IX. Application of the maximum likelihood approach to this data-set is bound to be misleading because the data have an apparent bias. The most suitable choice, then, is to pick $1-\sigma$ numbers that encompass all of the results. A $1-\sigma$ proportional magnitude (σ_2) of 0.2% and proportional pointing (σ_4) of 2 mrad (0.11°) covers all the errors. Navigation recommended changing the official model in Table II to these numbers so that they may be used for planning the remainder of the mission.

CLOSING

Early cruise for Cassini-Huygens program has been very successful. Delivery accuracy has been very good for each swingby and three maneuvers have been cancelled so far, with minimal ΔV cost. In fact, there has been an overall ΔV savings compared to pre-launch estimates. Analysis of the benefits from using the smaller execution error model is in progress. The ΔV savings is expected to continue.

Experience with the Cassini Spacecraft has been very successful and should lead to exciting science investigations of the Saturnian planetary system. Maneuver performance thus far has been nominal, and the team fully expects mission success to follow.

ACKNOWLEDGEMENT

The work described in this paper was carried out by the Jet Propulsion Laboratory, California Institute of Technology, under a contract with the National Aeronautics and Space Administration.

APPENDIX: THE B-PLANE

Planet or satellite approach trajectories are typically described in aiming plane coordinates referred to as “B-plane” coordinates (see Figure 11). The B-plane is a plane passing through the target body’s center and perpendicular to the asymptote of the incoming trajectory (assuming two-body conic motion). The vector \mathbf{B} is a vector in that plane, from the target body’s center to the piercing-point of the trajectory asymptote. The vector \mathbf{B} specifies where the point of closest approach would be if the target body had no mass and did not deflect the flight path. Coordinates are defined by three orthogonal unit vectors, \mathbf{S} , \mathbf{T} , and \mathbf{R} with the system origin at the center of the target body. The \mathbf{S} vector is parallel to the incoming V_∞ vector (approximately the velocity vector at the time of entry into the gravitational sphere of influence). \mathbf{T} is arbitrary, but is typically specified to lie in the ecliptic plane (the mean plane of the Earth’s orbit), or in a body equatorial plane. Finally, \mathbf{R} completes the orthogonal triad with \mathbf{S} and \mathbf{T} .

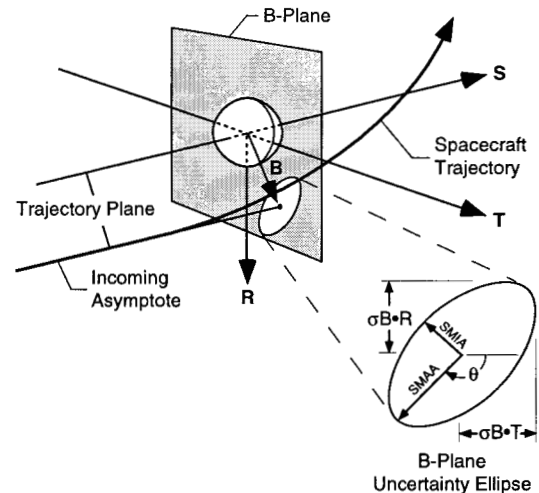


Figure 11: B-plane Coordinate System

Trajectory errors in the B-plane are characterized by a one-sigma ($1-\sigma$) dispersion ellipse, shown in Figure 11. SMAA and SMIA denote the semi-major and semi-minor axes of the ellipse; θ is the angle measured clockwise from \mathbf{T} to SMAA. The dispersion normal to the B-plane is typically given as a one-sigma *time-of-flight* error, where time-of-flight specifies what the time to encounter would be from some given epoch if the magnitude of \mathbf{B} were zero. Alternatively, this dispersion is sometimes given as a one-sigma distance error along \mathbf{S} , numerically equal to the time-of-flight error multiplied by V_∞ .

- 1 Gray, D. L., and Hahn, Y., “Maneuver Analysis of the Cassini Mission,” AIAA Paper 95-3275, presented at the AIAA/AAS Guidance, Navigation & Control Conference, Baltimore, Md., August 7-9, 1995.
- 2 Goodson, T. D., Gray, D. L., and Hahn, Y., “Cassini Maneuver Experience: Launch And Early Cruise,” AIAA Paper 98-4224, presented at the AIAA Guidance, Navigation, & Control Conference, Boston, MA, August 10-12, 1998.
- 3 Ionasescu, R., “Navigation Plan Update for October 15, 1997 Prime Mission”, JPL Internal Memo 312.A/024-98, October 2, 1998
- 4 Guman, M. D., “Navigation Plan Update for October 15, 1997 Prime Mission”, JPL Internal Memo 312.A/003-99, February 12, 1999
- 5 “Cassini Program Environmental Impact Statement Supporting Study. Volume 3: Cassini Earth Swingby Plan,” Internal Document 699-70-3, November 18, 1993.
- 6 Leeds, M. W., Eberhardt, R. N., and Berry, R. L., “Development of the Cassini Spacecraft Propulsion Subsystem,” AIAA Paper 96-2864, presented at the 32nd Joint Propulsion Conference, Lake Buena Vista, FL, July 1-3, 1996

-
- 7 Wong, E. C., and Breckenridge, W. G., "An Attitude Control Design for the Cassini Spacecraft," AIAA Paper 95-0713, presented at AIAA GNC 1995, Baltimore MD.
 - 8 Gates, C.R., "A Simplified Model of Midcourse Maneuver Execution Errors," JPL Technical Report 32-504, JPL, Pasadena, CA, October 15, 1963.
 - 9 Kopf, E. H., "EGA/EGE Performance during Cassini REA burns," JPL Internal Memo 344-99-002, December 21, 1998.
 - 10 Guman, M. D., Roth, D. C., Ionasescu, R., et. al., "Cassini Orbit Determination From First Venus Flyby to Earth Flyby," AIAA Paper 00-168, presented at the AAS Spaceflight Mechanics Meeting, Clearwater, FL, January 23-26, 2000.
 - 11 Lewis, G. D., "Earth Orbiting Debris Collision Avoidance During a Hyperbolic Flyby: The Cassini Experience," JPL Internal Memo 312.A/034-99, September 13, 1999.